DOI: 10.13009/EUCASS2017-654

Ground Ignition simulation methodologies for a cryogenic H_2/O_2 propellant fed rocket engine

Alban du Tertre, Laurent Gomet*, Cindy Merlin*, Dieter Hummel**, Didier Guichard*, Julien Guiraud*, Noel David*, Roland Behr***

**Airbus Safran Launchers - Vernon – France – cindy.merlin@airbusafran-launchers.com, alban.du-tertre@airbusafran-launchers.com, laurent.gomet@airbusafran-launchers.com, didier.guichard@airbusafran-launchers.com, noel.david@airbusafran-launchers.com*

***Airbus Safran Launchers - Ottobrunn – Germany – dieter.hummel@airbusafran-launchers.com, roland.behr@airbusafran-launchers.com*

Abstract

This study led by Airbus Safran Launchers aims at developing and validating a numerical approach to estimate the load generated by an external ignition on the thrust chamber assembly in case of non operating pyrotechnic igniter. In order to characterise these "ground ignition" loads and to evaluate the possible mechanical response of the various parts of the engine submitted to this transient load case, different computation tools with various degrees of complexity have been adapted (coupled gas-dynamic and mechanical computations) and compared to some experimental measurements carried out on the engine during failure-case test. Finally, the full computational workflow was able to, *a priori*, define a worst load case and simulate the mechanical response of the engine.

1. Introduction

The first stage of the European launcher Ariane 5 is built around the well known Vulcain 2.0 hydrogen-oxygen cryogenic engine. The main chamber of this gas generator cycle engine is ignited thanks to a pyrotechnical device. Nevertheless, in case of failure of this igniter, the burners located at the outlet of the nozzle extension of the thrust chamber assembly (TCA), usually aimed at igniting the preflow of hydrogen, can ignite the mixture flowing out of the TCA leading to an external ignition of the combustion chamber. Even if this scenario of ignition was never encountered in a flight configuration, it was investigated during the early development of the engine as a worst case scenario of the ignition and tested with a predesign of the nozzle extension. During this strongly deviated test, the nozzle extension evidenced some permanent deformation.

This study led by Airbus Safran Launchers aims at developing and validating a numerical approach enabling the estimation of the load generated by an external ignition from nozzle extension (NE) up to the cardan. In order to characterise the corresponding loads and to evaluate the possible mechanical response of the Thrust Chamber Assembly (TCA) submitted to this transient load case, different computation tools with various degrees of complexity have been adapted (coupled gas-dynamic and mechanical computations) and compared to some experimental measurements carried out on the engine during these failure-case tests.

For the mechanical aspects, several kind of modeling have been used with different software in order to first, validate the dynamic pressure loading simulations mentioned here-above and second, assess the effects of such a loading on the TCA. If, for the first of these two objectives, NE limited FE models are possible, the second aspect dealing with the global TCA behaviour, necessitates enrichments while remaining compatible with acceptable models sizes and realistic computation durations. Thus, one of the methodological challenges of this study was to be able to conclude on the possibility to use classical FEM codes to study the structural response to such rapid transient phenomenon which only lasts few milliseconds and to evaluate the axial effort generated on the cardan.

The development and validation of the computational workflow was performed in two steps. The first step was a validation of both the pressure load case, estimated thanks to a CFD approach, and the nozzle extension deformation, evaluated thanks to mechanical computations. This validation is presented in the Figure 1.

DOI: 10.13009/EUCASS2017-654

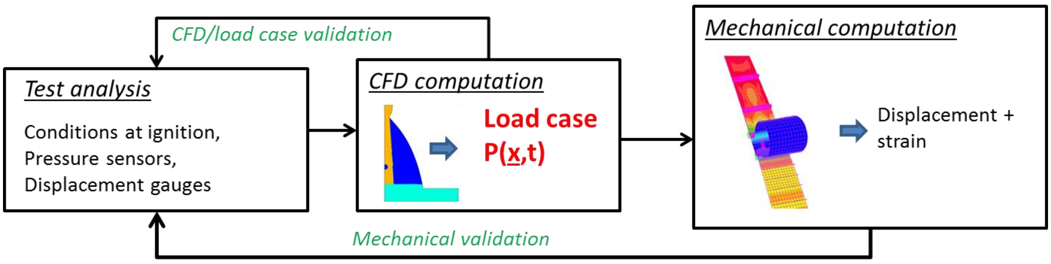

Figure 1: Summary of the computational workflow together with the validation of each methodological blocks

The validation of the numerical pressure field was made by direct comparison of the numerical pressure evolution with the pressure signal measured during the test. Before performing CFD computations, a physical analysis of the start-up transient was made to identify the main driving parameters which determine the initial conditions before ignition. Since all the parameters are not known accurately, a sensitivity analysis was performed and the results compared to engine test measurements in order to select the hypothesis of the simulation that fitted the best to the test sensors signals.
Once this pressure load was selected, it was applied to the mechanical model in order to compute the displacements of the structure and the generated strain. The response of the numerical model was then compared to the measurement acquired during the test.

This paper describes these two steps of validation. First, the CFD methodology is presented with all assumptions made to generate the load case called LC#1. Then, the mechanical model is presented and its response to the LC#1 is described. The third part gives an insight into the engine model and its behaviour under the LC#1. The second step of validation follows from fluid point of view with first the definition of a worst deviated case called LC#2 and then the estimation of the deformation induced by the LC#2 thanks to the mechanical model previously validated.

2. Computational Fluid Dynamics approach, definition of the LC#1

2.1 CFD methodology

The pressure load is generated thanks to N3S-Natur [3] which solves the three-dimensional compressible and reactive Navier–Stokes equations; it relies on a mixed finite volume (FV)=finite element (FE) approach applied on unstructured meshes made up of either triangular elements in 2D or tetrahedral elements in 3D. The use of the monotone upwind-centered scheme for conservation law (MUSCL) method combined with flux-limiting functions leads to a total variation diminishing (TVD) numerical scheme, yielding second-order spatial accuracy and avoiding the merging of spurious numerical oscillations in the vicinity of discontinuities. The limiting function of Van Albada et al[4]has been used here. The transport equations for mean density, momentum, total energy, turbulence kinetic energy, its dissipation rate and species mass fractions, are solved.

The turbulence closure relies on a k-epsilon approach with additional terms that take into account the compressibility effects of the turbulence [5]. In addition, special wall laws called LTM [6] are applied in order take into account the boundary layer in the nozzle extension.

The reacting flow was modeled by a one-step reaction due to Marathe et al.[7]. The production term follows the classical Arrhenius law

In addition, in order to avoid non physical temperature induced by a single step reaction, four gaseous species were considered in the computation: H_2, O_2, BG and N_2. BG (Burnt Gases) is a H_2O with modified specific heat in order to take into account the dissociation at high temperature and properly evaluate the burnt gases temperature.

Finally the resolution of this system of equations together with the previous closure allows carrying out a sensitivity analysis of the pressure load to the initial conditions of the computation.

DOI: 10.13009/EUCASS2017-654

2.2 Definition of the flow-field in the nozzle and parametrical analysis

The flow-field inside the nozzle extension before ignition is fully defined by five parameters:

- The pattern of the mixture inside the TCA,
- The composition of the mixture inside the TCA,
- The deflagration-to-detonation transition location,
- The pressure in the TCA,
- The temperature of the mixture.

The determination of these five parameters is based on some assumptions and experimental observations which are explained in the following. This study is performed with a 2D axisymetrical assumption which is relevant since the ignition point is located on the center line of the NE.

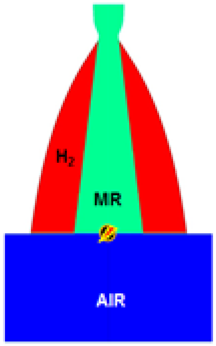

Pattern of the mixture in the TCA

The pattern of the mixture in the TCA is a parameter of first importance since it induces the direction in which the detonation wave can propagate and possibly be amplified. Regarding the volume occupied by the reactive mixture, two filling patterns can be reasonably considered as depicted in Figure 2.

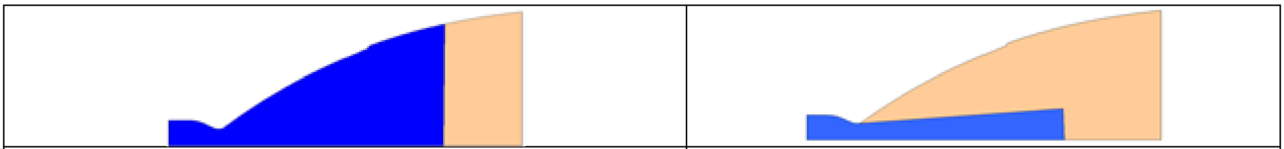

Piston-effect filling pattern	Cylindrical or conical filling pattern

Figure 2: Piston-effect and cylindrical/conical filling patterns

Detonation computations were performed with these two patterns in a parametrical analysis. It was found that the piston effect filling pattern wasn't able to reproduce a physical behavior. In addition, simplified two-phase flow simulations were carried out and results depicted in Figure 4 and Figure 5 show that the conical pattern is the most suitable. Finally, it is also interesting to note that during the start-up transient a dense phase can be seen on the center line at the exit of the NE, see Figure 3. This dense phase could be reasonably interpreted as a LOx flow. This tends to confirm that the mixture with oxygen is along the center line what is coherent with the conical filling pattern assumption. This assumption is also relevant with the natural "free fall" of injected fluids that can be expected in an outside winds protected area.

Figure 3 : Picture of the flow at the exit of Vulcain2 nozzle extension during ignition

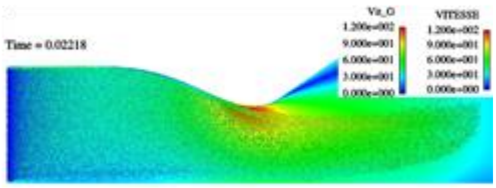

Figure 4 : Two-phase flow simulation, droplets and gaseous phases colored by their speed

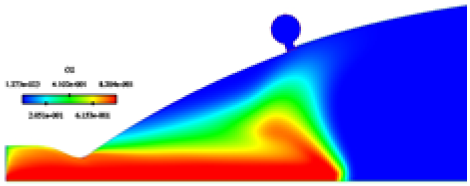

Figure 5: Two-phase flow simulation, mean flow-field of oxygen mass fraction during start-up transient

Once the pattern is assumed conical, the composition of the mixture must be defined. In order to have a limited number of parameters, the mixture inside the cone is assumed as homogeneous. It is obvious that this assumption

DOI: 10.13009/EUCASS2017-654

simplifies the real flow-field inside the nozzle but is chosen to easily control the mixture distribution in the NE. In addition, since the NE is full of hydrogen before opening the LOx chamber valve (VCO), the volume outside the cone and inside the nozzle is assumed to be pure hydrogen.
To fully determine the filling mixture pattern inside the nozzle extension, the length and the radius of the cone are still to be defined. From a parametrical analysis it can be concluded that the pressure wave amplitude increases with the radius of the cone and with its length. In order to maximize the pressure wave, and thus the load on the NE, the length and the radius of the cone must be maximized. Nevertheless, it must be noted that, for a given mixture ratio, the dimensions of the cone determine the quantity of oxygen in the nozzle extension, i.e. the energy introduced in the NE. That is the reason why, to determine a dimensioning load case the length and the radius of the cone must be as increased as possible but stay within physical limits.

Finally, it is assumed that the length of the cone is the length of the NE in order to maximize the energy inside the NE. The radius of cone is evaluated from the conservation of total mass of the mixture for a given quantity of oxygen and a given mixture ratio.

Mixture temperature

An important parameter, with regard to detonation, is the mixture temperature. It can be found in the literature [8] that the colder the mixture, the stronger is the detonation wave. This can be explained by the densification of the mixture which leads to an increase of the available energy before detonation. In order to maximize the energy available for detonation and derive a worst case, the mixture is assumed gaseous before ignition. Nevertheless, the oxygen is injected liquid (at least a part). That is the reason why the energy needed to vaporize the LOx is assumed to be taken from the gaseous phase. The temperature of the mixture is then estimated with:

- Temperature of O_2 at injection of 100K
- Temperature of H_2 at injection of 190K
- O_2 vaporization heat of 207kJ/kg/K

These assumptions allow us to plot the evolution of the mixture temperature as a function of the mixture ratio. This evolution is depicted in Figure 6 for two different proportions (mass fraction) of liquid O_2 at injection plate level.

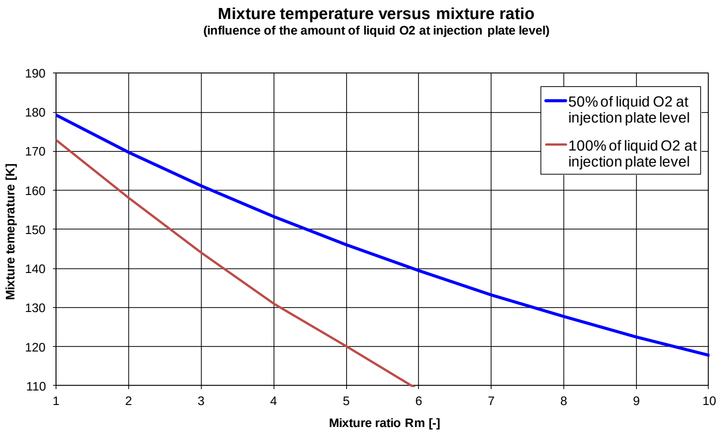

Figure 6 : Mixture temperature versus mixture ratio for two different mass fractions of liquid oxygen at injection

From this figure, if the proportion of liquid oxygen is chosen, 50% of liquid and 50% of gas is the blue curve is considered, the mixture temperature is fully defined from the mixture ratio.

Determination of the mixture ratio

As found in the literature [8], the closest the MR is from the stoichiometry, the stronger the detonation wave is. Nevertheless, for the same amount of oxygen, the higher the MR is, the smaller the cone radius is. So, there is competition between these two phenomena in our configuration.
The conjugated influence of these two parameters is evaluated, for the same amount of oxygen inside the nozzle extension, for a mixture ratio of 4 and a mixture ratio corresponding to the detonation limit for a H_2/O_2 mixture. An illustration is plotted in Figure 7.

DOI: 10.13009/EUCASS2017-654

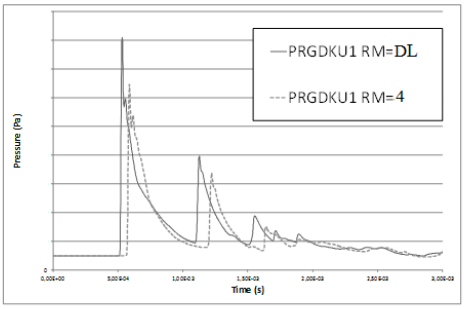

Temporal evolution of the pressure at X=1.001903m

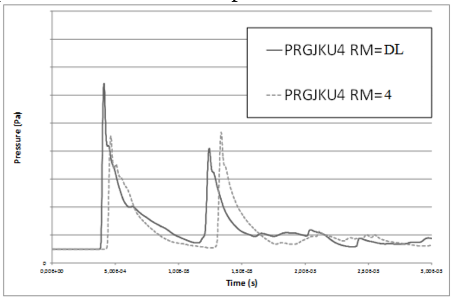

Temporal evolution of the pressure at X=1.737903m

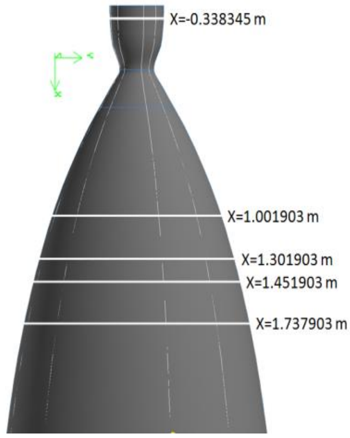

Figure 7 : Illustration of the conjugated influence of mixture ratio and cone radius on pressure evolution for two different sensors (DL corresponds to the detonation limit)

From these results it appears that the cone radius influence is of first order compared to the MR influence. This conclusion leads to choose the smallest value of the MR in order to maximize the radius of the cone inside the nozzle and then maximize the pressure load.

Determination of the amount of oxygen in the TCA

Finally, following the previous analysis, the initial distribution of the mixture in the TCA leading to a worst case is only driven by the amount of oxygen inside it prior to ignition. Nevertheless, the determination of this amount of oxygen is quite complicated since some oxygen could flow out of the nozzle extension before ignition of the chamber. In a worst case approach it can be assumed that all the oxygen is trapped in the TCA before ignition, thus the amount of oxygen can be estimated either thanks to a system simulation or from test measurements.

Determination of the location of the initiation point

In reality, in case of igniter failure, combustion reaction is initiated by ground burners leading to propagation of a flame and, in a worst case approach, a transition from deflagration to detonation. Since the computation of this transition is quite complicated and, nowadays, still is an open point, it is chosen in a worst case approach to directly prescribe a Chapman-Jouguet state (see [8]) and thus, ensure the mastering of the initial detonation location.
With this approach, the worst case is obtained with a detonation initiated at the bottom of the nozzle extension.

2.3 Validation of the computational workflow, determination of the LC#1

As stated previously, a test of external ignition was performed with a specifically instrumented engine. Among the sensors implemented on this hardware (H/W), 3 pressure sensors were added to the nozzle in order to measure the evolution of the pressure along the internal profile during the transient startup of the engine. To validate the full computational workflow, the first step is to define a pressure load corresponding to the test. However, even if the previous sensitivity analysis allows us to define a worst case for the initial condition, it is not possible to easily reproduce the initial conditions relevant of a test environment because all parameters are still degrees of freedom.

DOI: 10.13009/EUCASS2017-654

That is the reason why it was chosen to perform many computations with various initial conditions and select the ones that generate the pressure field that fits the best the pressure signal from the sensors.
The result of the computation which fit the best the experimental measurements is presented in the Figure 8.

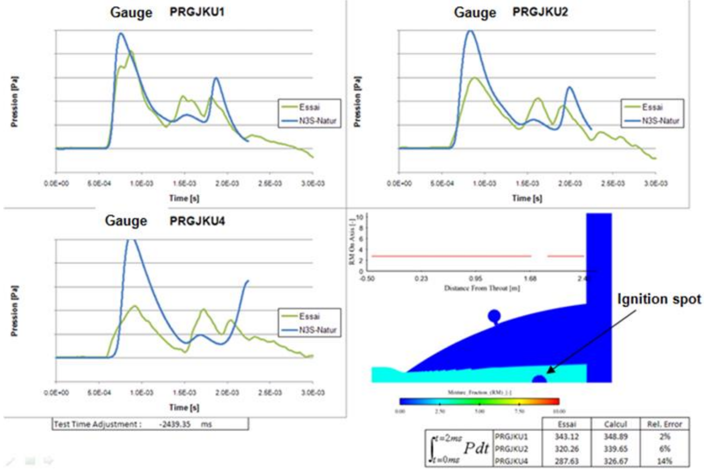

Figure 8 : pressure load case LC#1: hypothesis & fit on the pressure measurements.

On these graphics it can be seen that for this LC#1 load case, the width of the pressure peaks as well as the temporal aspect are quite well reproduced: the 3 pressure peaks are correctly positioned and the amplitude computed fits quite well with gauge PRGJKU1 measurement. Even if the pressure amplitude computed for gauge 2 and 4 overestimates the measurement, the width of these peaks is correct and the 3 peaks are present for the 3 gauges. The minimum values are also well positioned.
Once this pressure load case is defined, its effect on the structure can be estimated thanks to the mechanical model of the TCA. This step is described in the following part.

3. Tuning and validation of the symmetrical load case LC#1

The mechanical model described here is the final result of several development activities carried out at Airbus Safran Launchers (formally Safran Snecma) since 2004. At the beginning, studies started with a simple 2D axisymetric model of Vulcain 2.0 predesign NE that rapidly evolved towards 1/30th 3D model of the Vulcain 2.0 final design including the complete TCA [1]. Later on, new improvements were implemented like taking the high strain speed effects on the materials hardenings behaviours as well as the gravity acceleration into account.

Thus, in 2006, a high strain speed material characterization campaign (tension tests) has been carried out for Inco 600, Hastelloy X and Haynes 230 (room temperature, strain speeds up to 300 s^{-1}) and Symonds Cowper law has been implemented into Samcef™ Mecano in order to take this dynamic aspect on materials into consideration. Parameters D & P of this law (1) have been identified for the average natural hardening curves of the three materials. The quasi-static hardening curve is multiplied by a function of the strain speed as follows:

$$\sigma_{dyna} = \sigma_{stat} \left[1 + \frac{\dot{\varepsilon}_{pl,eq}}{D} \right]^{1/P} \tag{1}$$

Finally, in 2010 a dedicated validation engine fire test campaign was carried out to validate the complete improved mechanical model on LC#1. For that purpose, different strain gauges have been implemented on the NE to measure total mechanical strain evolutions during the shock close to the identified most solicited areas of the structure.
Four strain gauges were welded on the NE (cf. Figure 9). Two gauges were vertically oriented (meridian direction): KPTRA7 in the plane containing LEH (Exhaust Line from H_2 turbopump) and KPTRA8, in an area not affected by exhaust lines. The two other gauges were horizontally oriented (hoop direction): KPTRT2, and KPTRT3.

DOI: 10.13009/EUCASS2017-654

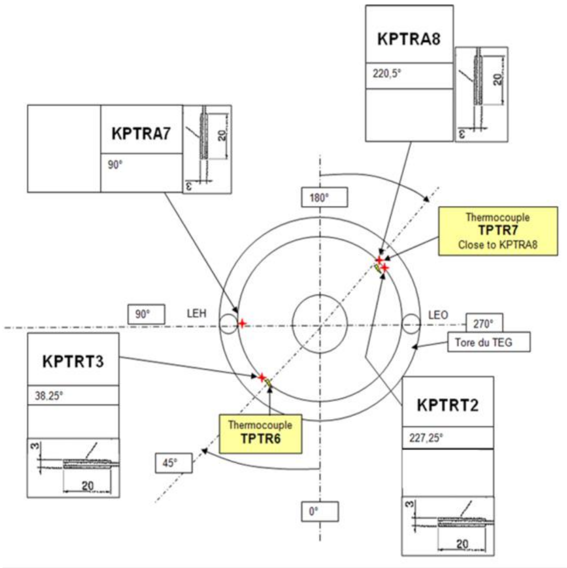

Figure 9:Angular positions & orientations of strain and temperature gauges around Vulcain 2.0 NE (from above).

The FEM model was the following:

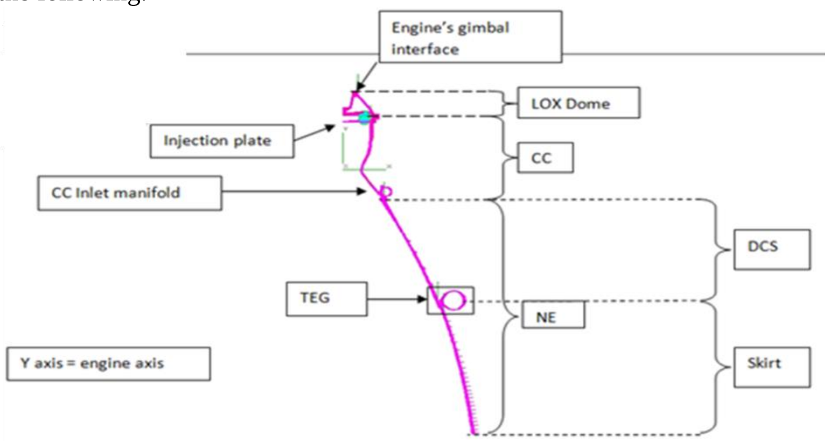

Figure 10 : Vulcain 2.0 NE 1/30th 3D FEM.

The structure is fed with a temperature profile representative of the thermal steady state at ignition. The simulation lasts for 50 ms. Computation time steps are reduced (5E-4s) during the first 5 ms. In order to rapidly end the computation with a structure in a steady state, a numerical Newmark scheme damping is implemented significantly after the shock (from t= 30ms to t=50ms) to prevent the structure from vibrating indefinitely. This damping does not affect the final deformation of the structure. The comparison between simulations and measurements are detailed hereafter.

The following graph shows the comparison between calculation results (dash lines for the four adjacent post-treated elements) and experimental signals (plain blue & red curves) from KPTRT2 & 3 horizontal (circumferential) gauges. Plain red curve is the computed average strain over the 4 post-treated elements.

DOI: 10.13009/EUCASS2017-654

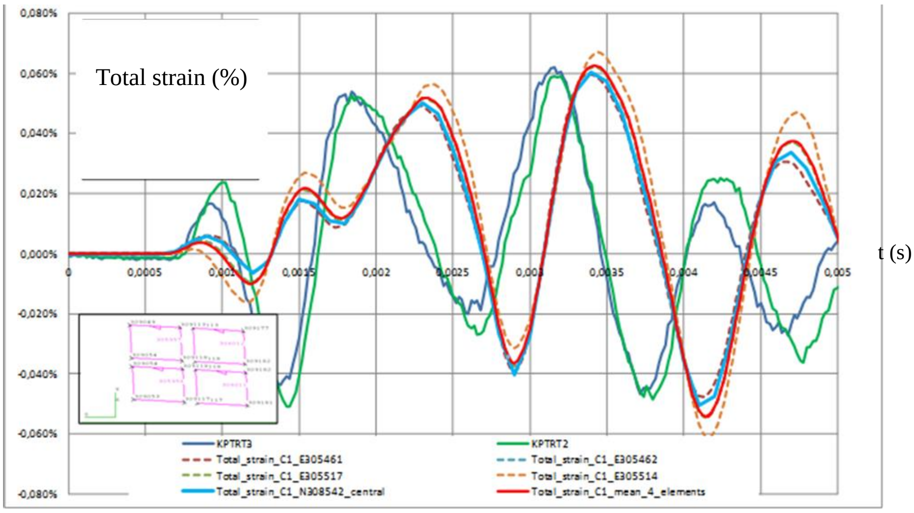

Figure 11: Components 1 of total natural strain tensor of the elements compared to experimental signals from KPTRT2 & 3 gauges (dark blue and green).

Concerning the gauges signals (dark blue & green) what is striking is that they are almost superimposed whereas they were measured at 180° from each other. Considering the average gauges signal is thus a good reference to take the 3D aspect of the phenomenon into account. Concerning the simulations, we can observe that the maximum amplitude of the average total strain computed on the 4 FE (red curve) during these first 5 ms fits exactly (1 to 1) to the experimental measurements. The strain evolutions of each FE are also very close to this average curve. The frequencies of the computed evolutions of the mean total strain and of the experimental signals are in good agreement (see frequency analysis further).

If we now consider the experimental signals from KPTRA8 vertical (meridian) gauge, we obtain:

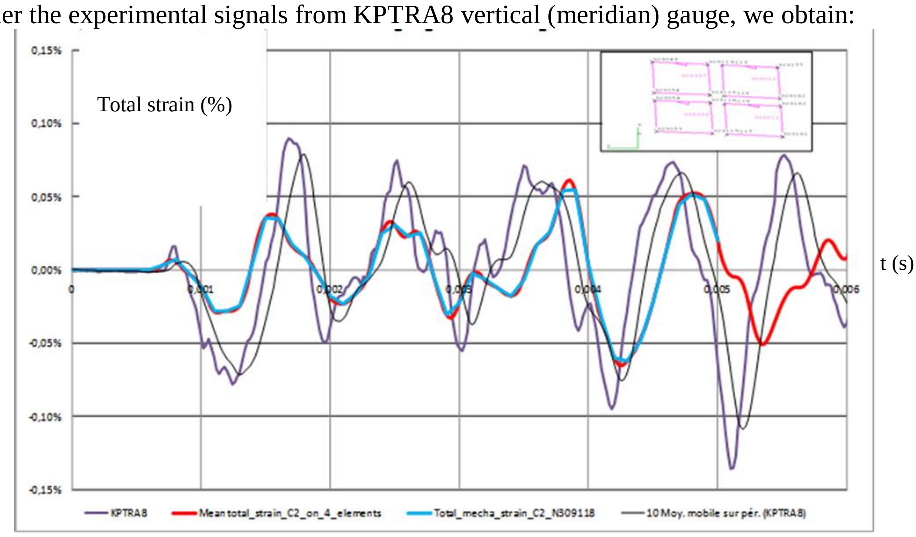

Figure 12: Average component 2 of total natural strain tensor of the elements (red) compared to experimental signal from KPTRA8 gauge (purple and black = mobile mean).

On this graph we can also observe that the maximum amplitude of the average total strain computed during these first 5 ms fits almost exactly (1 to 1) the experimental measurement, especially if we consider the mobile mean of the KPTRA8 signal out of 10 values (black curve). The frequencies of the computed evolutions of the mean total strain and of the experimental signal are in good agreement (see frequency analysis here-under).

For both circumferential and meridian gauges, the temporal aspect and notably the frequencies of the total strain evolutions have bee analyzed. A shock response spectrum analysis of the experimental and computed total strain signals has been carried out with the Scilab 5.0.1 software in order to determine a representative frequency of the signals which could constitute a relevant comparison basis. This determination is not as easy as it seems since both experimental and computed signals are not perfect periodic signals and their frequency is not constant as time passes.

DOI: 10.13009/EUCASS2017-654

For this reason, the chosen strategy consisted in using a shock response analysis on previously filtered signals (the high frequencies above 2 kHz are suppressed).

The filtered signal to analyze is considered as a "temporal shock signal" and is applied on a 1 degree of freedom (D.O.F.) spring-mass system whose eigen frequency is known. This 1 D.O.F. system will have its own response characterized by its maximum value. This maximal value is kept and plotted in graph vs. the eigen frequency. By changing "n" times the eigen frequency of the 1 D.O.F. system, "n" maximal responses are obtained which, together, give a shock response spectrum. The frequency corresponding to the maximum response of the spectrum is the result given by the software. This method is very well adapted in our case since it allows to extract the most representative frequency contained in the experimental and computed total strain signals. The frequency thus extracted will constitute a relevant indicator of the good temporal fit of the model w.r.t. the experimental measurements. As an example, the obtained results are shown on Figure 13 for circumferential gauges 2 and 3:

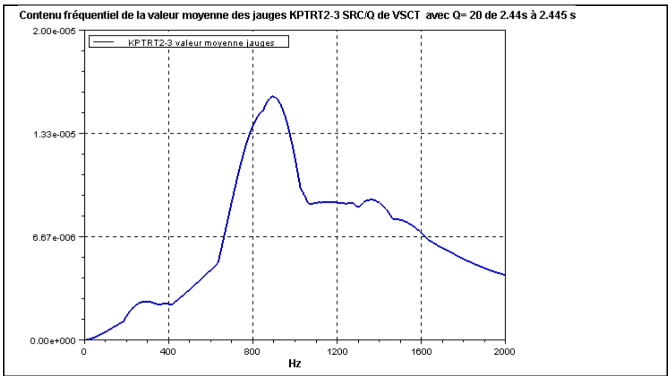

Frequency content of the experimental signal
Maximum response frequency : 895Hz

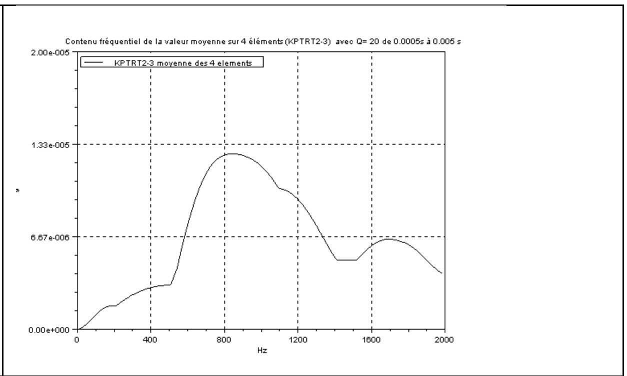

Frequency content of the computed signal
Maximum response frequency : 836 Hz

Figure 13: Frequency analysis of mean signal from KPTRT2&3 gauges on the first 5 ms

The same methodology was used for the meridian gauges and the final results are given in the table below:

Table 1: Frequency fit between experimental and computation

	Circumferential gauges	**Meridian gauges**
Gap fit (relative)	6.6%	7.3%

The gap is small. The temporal fit is satisfactory in both directions. Since the modelization correctly fits both experimental total strain amplitudes and frequencies it is chosen not to apply any tuning coefficient on load case LC#1. This study shows that the 3D 1/30th cyclic-symmetrical model of the Vulcain 2.0 TCA is able to correctly simulate the structure's response to a rapid transient evolution of the inner pressure and is thus validated. The complete "effort chain" from the lower end of the skirt to the cardan interface is taken into account which allows to determine the axial resulting effort at different interfaces between the TCA main components. This is important since the stiffness of the structure evolves along the axial engine axis.

Main conclusion of this first application of the computational workflow to a specific test is that, if the initial conditions of the computational fluid dynamics simulation are relevant w.r.t. the initial conditions of the test, the workflow is able to correctly assess the right displacement of the nozzle extension.

4. Assessment of mechanical effects of LC#1 on the whole TCA

The established methodology is so able to evaluate the mechanical impact of external ignition onto the nozzle extension. The impulse generated by the detonation is upon that transmitted to the neighbouring components, the combustion chamber, the cardan and associated actuators and the launcher thrust frame.

DOI: 10.13009/EUCASS2017-654

As the detonation can be assimilated to a shock, the aim of a global engine simulation is to analyse the shock response and its mechanical impact on the listed components. In order to fit to the real hardware, the dynamic behaviour of the engine shall be correctly represented in terms of Eigen frequencies, which means that all masses, stiffnesses and inertias shall be implemented in the FE model. Also, the shock response analysis implies a time dependant simulation with a quite high number of time steps. For comparison with test bench results, the launcher thrust frame has been replaced by the test bench thrust rig (Figure 14).
For these reasons, a simplified but complete engine model has been established, taking into account for turbomachinery, gas generator, electro-valves box support and test bench thrust rig.

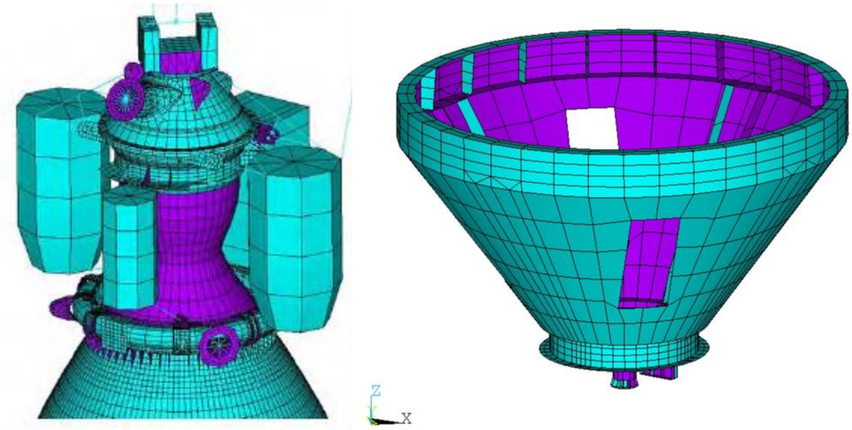

Figure 14: simplified FE engine model and thrust rig.

When discussing about dynamic response in FEM computation, one question regards the dynamic damping value to be used. A Rayleigh damping model was used and calibrated on test results, thanks to the accelerometers fixed close the cardan interface. This model offers the advantage to propose a frequency dependant damping factor on a large frequency range from 500 to 800Hz.
For direct comparison with test results, the outputs used from these computations are time dependant displacements and accelerations at each node of the model.

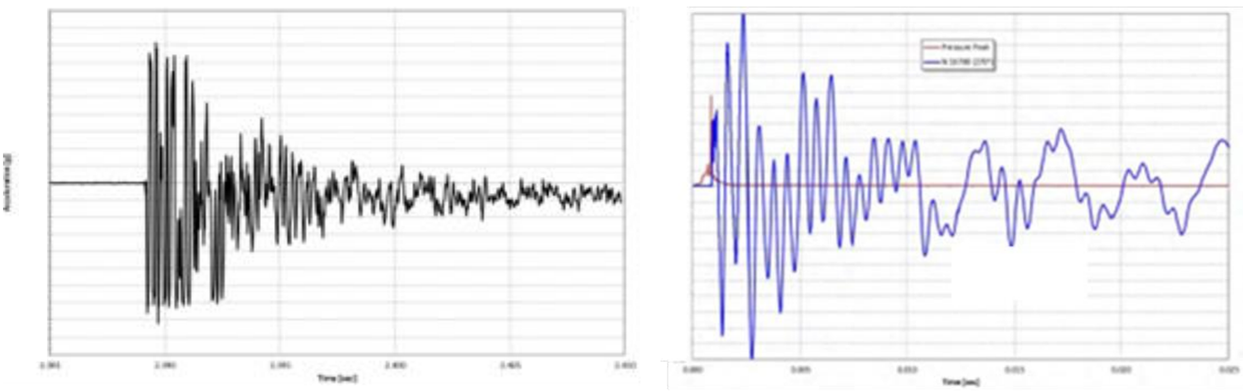

Figure 15: measured (left) and computed (right) accelerations on TCA Red= pressure peaks evolution.

A comparison of dynamic response computation, using the thrust chamber (including the cardan) alone, thrust chamber + thrust rig, thrust chamber + thrust rig + equipments, has demonstrated the necessity to implement a fully representative model, as a factor up to 3 on the results was found between the first thrust chamber model alone and the fully representative engine model.

Another kind of output are obviously the time dependant stresses in the Nozzle Extension and Combustion Chamber, and time dependant loads transmitted to the cardan, the engine actuators and the thrust rig, which gives all needed information for a full diagnosis on the engine

DOI: 10.13009/EUCASS2017-654

5. CFD Assessment of the LC#2 "worst case" loading

As presented in the previous part, the first step of validation is performed, demonstrating the capacity of the computational workflow to correctly simulate the response of the structure to a pressure load. The second step of the validation is the definition of an *a priori* worst case in order to compare the computed deformation to the one obtained after the strongly deviated test performed during the development of Vulcain2.0. This strongly deviated test was performed with tangential burners instead of radial burner leading to a very late ignition of the pre-flow of hydrogen and an outside air detonation (OAD).
From the parametrical analysis previously presented, an initial condition of the flow-field that generates a worst case loading can be defined.

- The pattern of the mixture is conical,
- The mixture ratio in the cone is 1.78,
- The DDT location is at the outlet of the NE,
- The pressure in the TCA is 1bar,
- The temperature of the mixture is 170K.

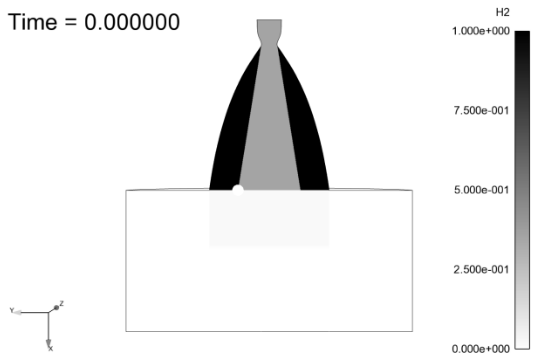

In addition, due to the tangential orientation of the burners, a mixture of hydrogen and air was located at the outlet of the NE. In a worst case approach, the OAD is simulated by a stoichiometric mixture of hydrogen and air in the grey rectangle.

The last open point of the initial condition is the location of the DDT point. Since the deformation of the nozzle extension after the strongly deviated test was not symmetrical, it is obvious that the pressure load was not symmetrical either. That is the reason why for the LC#2, the DDT point is not put in the centerline of the nozzle but at the boundary of the H_2/O_2 mixture. For this unsymmetrical initial condition the computation is performed on a 3D domain.
The propagation of the pressure wave obtained during the simulation is depicted on the following figure.

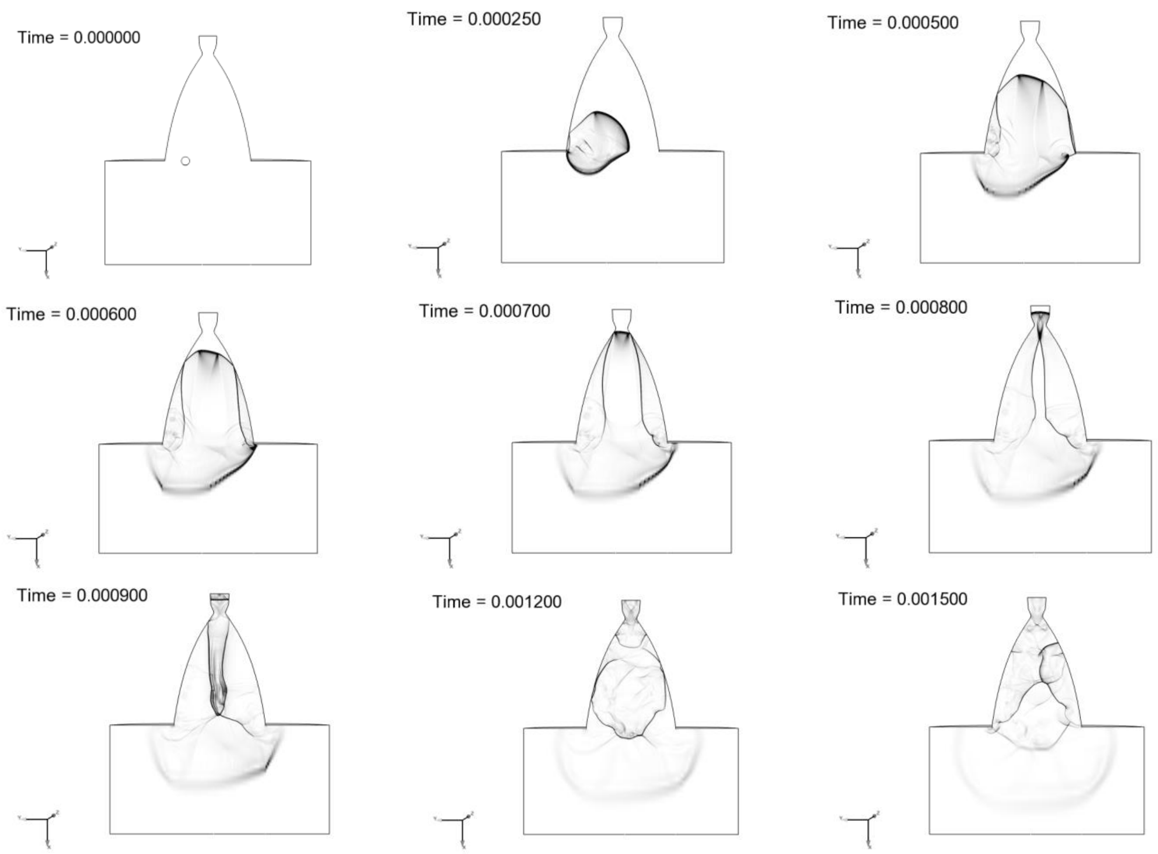

Figure 16 : Temporal evolution of a numerical schlieren of the pressure (grad(P)) for the LC#2

DOI: 10.13009/EUCASS2017-654

6. Tuning and validation of the unsymmetrical load case LC#2

The so called LC#2 worst load case has then been applied on a FE modelization of pre-design of Vulcain 2.0 NE This pre-design was a non flight worthy prototype on which such a degraded load case due to wrongly orientated ground burners was encountered during a fire test. Special venting was also deliberately imposed during this test to force the occurrence of this severe load case which is unsymmetrical and also include OAD phenomenon. As some measurable deformation was observed on this H/W, this test offers the ideal opportunity to validate both functional and mechanical methodologies.

As LC#2 is an unsymmetrical pressure load case, a complete 180° FEM of the NE was necessary to correctly map it on the structure. Symmetry boundary conditions (BC) are implemented in the symmetry plane. The model is shown on Figure 17 below:

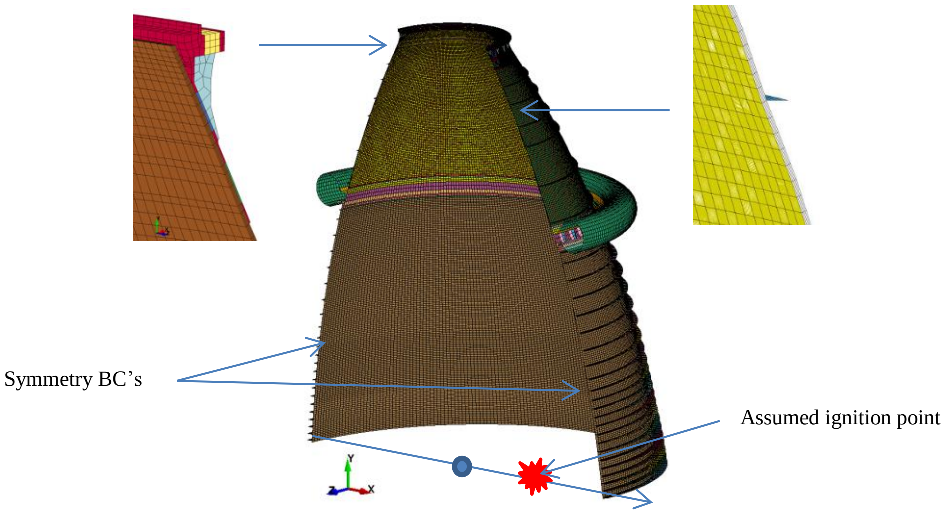

Figure 17: 3D 180° FEM model & BC's for LC#2 studies. Vulcain 2.0 pre-design NE.

As model size is large (~181000 nodes) and the pressure field complex, it has been necessary to go back to an explicit modelization scheme and to switch to LS Dyna™ code to obtain convergence. To compensate the more reduced number of integration points, some meshing refinements (more elements in the wall thickness) have been added w.r.t. the mesh used in the implicit scheme used so far with Samcef™ Mecano. Checks of energies balance have been performed, in particular Hourglass energy which shall remain low w.r.t. internal system energy.

Relative pressures fields are described this way: the NE is divided into fifteen 12° angular sectors. Each sector is axially divided into 252 "slices" from CC/NE interface to NE exit plane, each slice corresponding to a 1 element line. Each sector of a given slice is mapped with a time dependent relative pressure evolution function Pr(t).In a sector, linear angular interpolation is made from one function to the other. As an example, for a given slice, 5 of these pressure evolutions at different angular locations are shown in Figure 18 below.

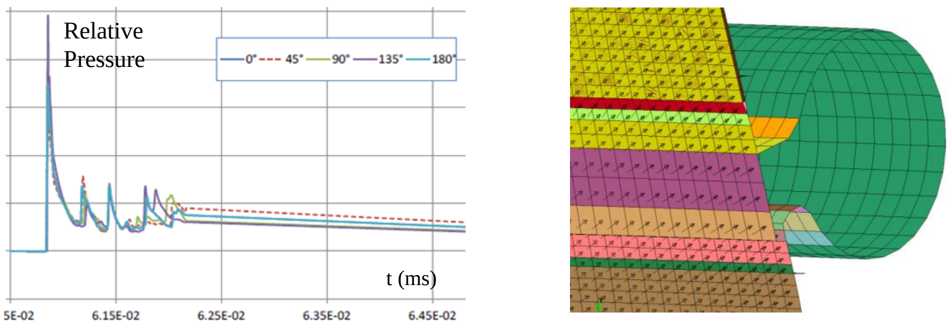

Figure 18: LC#2 pressure loadings (Unsymmetrical with OAD) for a given axial slice in the upper part of the NE @ different angular positions.

DOI: 10.13009/EUCASS2017-654

As for the computations made with LC#1 (cf. §3), a representative axial temperature evolution representative of ignition steady state is imposed on the NE as well as a pre-deformed 2D meridian profile that was measured before the validation fire test performed. Dynamic effects on materials hardening curves are also taken into account thanks to the Symonds-Cowper model (1). As far as inertia effect are concerned, they are also well taken into account by LS-Dyna.

As the main deformation observed on this pre-design non flight worthy H/W after the degraded test was a 360° angular evolutive “bump”, the main results were focused on residual structural displacements and plastic strain in the concerned area. By applying a limited 0.73 tuning factor on the LC#2 load case pressures, a good fit was obtained between computation results and H/W measurements. Figure 19 below shows for instance the computed evolution of the bump “height” during the ignition and the final value considered to define the loading tuning value which was finaly found at 0.75 to fully fit the measurements.

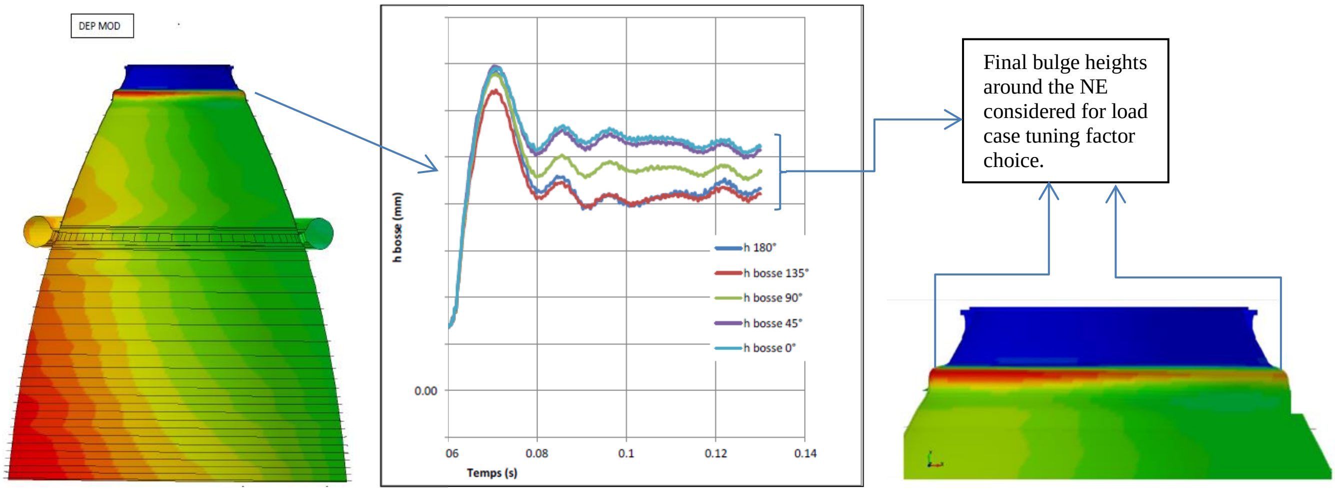

Figure 19: Computed displacements (modulus) and 360° bump heights used for LC#2 tuning factor choice. Tuning factor applied here is 0.73 on LC#2 unsymmetrical load case including OAD phenomenon.

Unsymmetrical aspect of the observed deformation is moreover very well represented by the computation.
For what concerns plastic strain a maximum 15% value is computed which is also in line with the bulge height observed on the H/W. It is show on the picture below for internal hot gas wall (HGW).

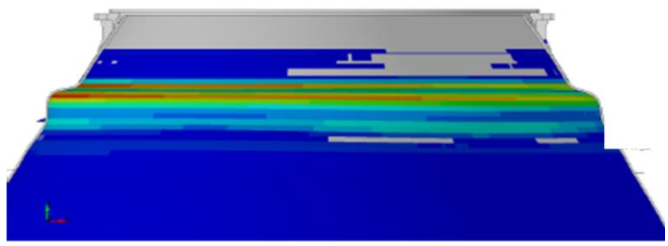

Figure 20: Computed plastic strain HGW. Tuning factor 0.73 on LC#2 unsymmetrical + OAD phenomenon.

Thanks to this works ASL has now a complete fluid-mechanical methodology to fully modeled such a voluntarily degraded “worst case” LC#2 due to wrong ground burners orientation and deliberated aggravating non flight like venting of the engine.

DOI: 10.13009/EUCASS2017-654

7. Conclusion

This paper describes the studies performed in order to develop and validate a computational workflow able to estimate the dynamics response of a thrust chamber assembly in case of non operating pyrotechnic igniter and external ignition of the thrust chamber. To achieve this, a CFD methodology is proposed based on a physical analysis and the pressure load generated by this computation is anchored thanks to the measurement performed during a failure test on engine. The mechanical model uses the time dependant pressure wave as input and its response to the CFD load case is analysed and compared to the behaviour of the engine during the failure test. This approach validates the computational workflow. The workflow is then applied to an extreme worst case loading and estimates the deformation of a pre-design of the Vulcain 2.0 nozzle extension. The deformation obtained is comparable to the one observed during a voluntarily degraded worst case test thanks to a moderate tuning factor.

Finally, this work enables now ASL to estimate a dimensioning load case that can occur in case of failure of the igniter and to give a full diagnosis on the engine.

References

[1] S. Sagnier, A. du Tertre 2007. High frequency Dynamic response computation with Samcef™ Mecano. Samtech Samcef Users conference. Liège (Belgium).
[2] Manuel des Techniques de l’Ingénieur
[3] R. Martin, D. Chargy 2001. Projet N3S-Natur, Manuel théorique. SIMULOG
[4] G.D. Van Albada et al. 1982. A comparative study of computational methods in cosmic gas dynamics. Astronomy and Astrophysics 108.
[5] O. Zeman 1990. Dilatation dissipation: the concept and application in modeling compressible mixing layers. Physics of fluids A: Fluid Dynamics, vol2.
[6] Daribeau F. 2002. Etude des transferts de chaleur aux parois dans les moteurs fusees.PhD Thesis.Institut national polytechnique de Toulouse.
[7] A.G. Marathe, H.S. Mukunda and V.K. Jain, Some Studies on. Hydrogen-Oxygen Diffusion Flame, Combustion Science and. Technology, 15, p. 49, 1977. 12.
[8] R.Borghi M.Destriau 1995. *La combustion et les flammes.* Ed. Technip.